Folded-Resonator Design of Thin-Disk Laser with Variable Thermally-Induced Intra-Cavity Dioptric Power

Saeid Radmard[a], Ahmad Moshaii*[a] and Mohammad Abazari[b]

[a]Department of Physics, Tarbiat Modares University, Tehran, Iran.
[b]Iranian National Center of Laser Sciences and Technologies, Tehran, Iran.

Corresponding author email: moshaii@modares.ac.ir

Regular paper: Received: Jul. 05, 2022, Revised: Oct. 16, 2022, Accepted: Oct. 16, 2022,
Available Online: Oct. 18, 2022, DOI: 10.52547/ijop.16.1.69

ABSTRACT— This paper presents the design procedure of folded-resonators for high-average power thin-disk lasers (TDLs). Because of the oblique angle of incidence in the laser path inside the resonator, folded resonators introduce astigmatism. Additionally, the dependency of the dioptric power of the active medium on the pump power made the resonator design more complicated. In the first section of this work, the disk thermal lensing was measured using a wavefront sensor, and the measurement procedure was presented and thoroughly discussed. The disk radius of curvature varied between 4.3 m to 6.4 m depending on the pump power. The disk was considered a variable lens inside the resonator based on the measurement results. V-shaped and L-shaped configurations' stability and M^2 factor were predicted, optimized, and compared. Astigmatism in the resonator parameters was considered and discussed. While the V-shaped cavity has better beam quality, the L-shaped cavity has less sensitivity to cavity misalignment. The primary approach of this paper was the resonator design of a cavity-dumped disk laser. However, the designed resonator configurations could be utilized in many laser resonators, such as industrial TDLs (to reduce the overall length of the system) and second harmonic-generation in TDLs.

KEYWORDS: Cavity-dumping, Folded-resonators, Thermal lensing, Thin-disk laser.

I. INTRODUCTION

Laser pulses with durations of tens of nanoseconds and multi-hundreds of watts average power have many applications in the industry [1-3]. Nowadays, pulsed lasers with average powers up to kW range can easily be obtained without the need for complicated oscillator-amplifier systems by thin-disk oscillators [4]. Generally, in solid-state lasers, pulses with tens of nanoseconds durations can be produced by the Q-switching method [5, 6].

Nevertheless, in thin-disk lasers (TDLs), the resonator length is relatively long, and the gain coefficient is low. So, the pulse duration in the orders of ten nanoseconds is not possible by the Q-switching method in TDLs. [7]. Additionally, Q-switching in low-gain lasers suffers from pulse-to-pulse instability, and the pulse energy bifurcation restricts the maximum repetition rate of the laser [8, 9]. This is a common problem in solid-state lasers and appears as a real issue in low-gain media such as TDLs [10]. Therefore, the maximum extractable average power of the Q-switched TDLs is limited.

In TDLs, pulses with multi-ten nanoseconds durations are produced by the cavity-dumping technique [11-14]. Contrary to Q-switching, which is based on loss modulation of the resonator, cavity dumping relies on the modulation of the laser output coupler transmission. In cavity-dumping, all resonator mirrors are high reflection (HR), and the output coupling is achieved by using an electro-optical modulator (EOM) with a thin film polarizer (TFP) as the laser output mirror.

This results in straightforward control of pulse durations [6].

However, in cavity-dumping, the polarizer is commonly placed at Brewster's angle in the resonator. So, the resonator configuration needs an oblique folding angle. This folding-resonator configuration is utilized in industrial lasers to reduce the overall length of the system, second harmonic generation, and mode-locked lasers. Astigmatism in the resonator characterization, such as transverse modes size, stability, and M^2 factor, is the drawback of folded resonators and must be compensated by the resonator design [15]. In addition, in TDLs, the dioptric variations of the active medium during pumping [16, 17], made the folded-resonator design procedure more complicated.

This paper presents a folded-resonator design procedure applicable in a cavity-dumped high average power TDL. In the design procedure, considerations and requirements of an industrial laser have been considered. The resonator must have a proper beam quality factor, reasonable geometrical dimension, and enough stability against mechanical vibrations. Additionally, astigmatism, due to the oblique angle of incidence in the resonance path, has been considered and discussed.

The first step of the resonator design was determining the thermal lensing dioptric power in all of the pumping powers. Measurement of thermal lensing by wavefront sensing had been mentioned in the literature. However, it had not been fully described, so here, the measurement procedure of thermal lensing of a TDL has been thoroughly discussed experimentally.

Considering the disk as a variable lens in the resonator, and based on the measured data, two kinds of folded-resonator configurations have been designed, investigated, and optimized. The Laser Cavity Analysis and Design (LASCAD) software has been used in this investigation. Resonators' stability region and beam quality factor have been analyzed and compared for these resonator configurations.

II. Measurement of Variable Dioptric Power of the Disk

The influential factors which change the disk's radius of curvature during the pumping process have been thoroughly discussed in the literature [16-18]. Whatever the source of these factors is, these lead to an effective pump-dependent radius of curvature for the disk. Based on the measurements, the disk's surface could be approximated as a spherical surface and treated as a variable thermal lens inside the resonator [17].

Our experiments utilize a TDL gain module designed and fabricated in the TDLs laboratory of INLC. The active medium is a Yb:YAG thin disk with a thickness of 200 μm and a doping concentration of 9 percent. The disk is bonded on a Cu-W cold-plate, and a jet-impingement water cooling system removes the heat from the disk. The pump source of the system is a stack diode-laser with continuous wave output power up to 1.4 kW. The gain module is specifically designed to fulfill the final aims of this work. Details and design procedures of this gain module have been fully discussed in our previous publications [19-21].

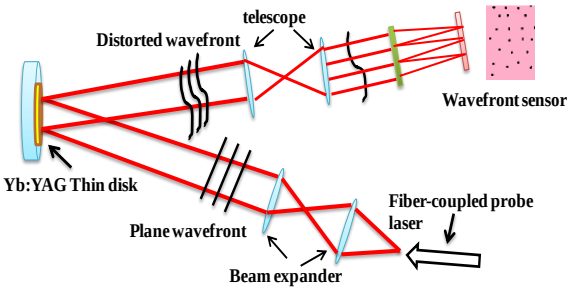

Fig. 1. Schematic of the setup used for measurement of the disk's radius of curvature.

A schematic of the measurement arrangement of the disk thermal lensing is shown in Fig. 1. As shown in this figure, the setup consists of a fiber-coupled diode laser (as the probe beam) and a beam expander (to produce a plane wavefront of the probe). A wavefront sensor (WFS) mounted on a telescope measures the reflected beam from the disk surface. Using the telescope, the distorted wavefront, after reflection from the disk's surface, is directed into the WFS, and the sensor measures its curvature.

In the measuring setup, the reflection of a plane wavefront from the disk surface has been detected by a Shack-Hartmann WFS and analyzed by Zernike polynomials. We approximated the disk's surface as a spherical surface and, considering the telescope's magnification, transformed the measured data to the disk's radius of curvature.

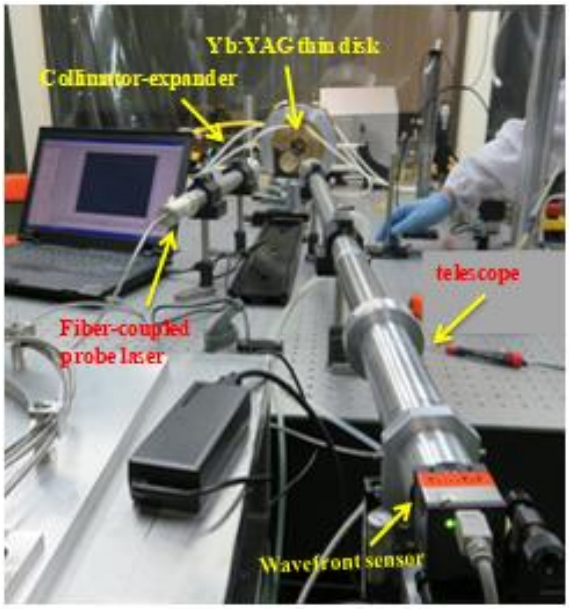

Fig. 2. The experimental setup used to measure the disk's radius of curvature.

The experimental setup to measure the disk's radius of curvature is shown in Fig. 2, and the results are plotted in Fig. 3. The WFS used in this procedure measures the reflected wavefront's curvature from the disk surface. An ideal flat wavefront beam reflected from a surface with a radius of curvature R is focused on the focal point, so the reflected wavefront curvature is $R/2$. To convert the measured value from the wavefront sensor to the disk radius of curvature, considering the optical magnification of the telescope, we have used the following relation:

$$R = 2 \times R_{WFS} \times M_{Tel} \qquad (1)$$

where R_{WFS} is the measured values of radius on WFS in millimeters, R is the disk's radius of curvature, and M_{Tel} is the telescope magnification, which equals 14.06.

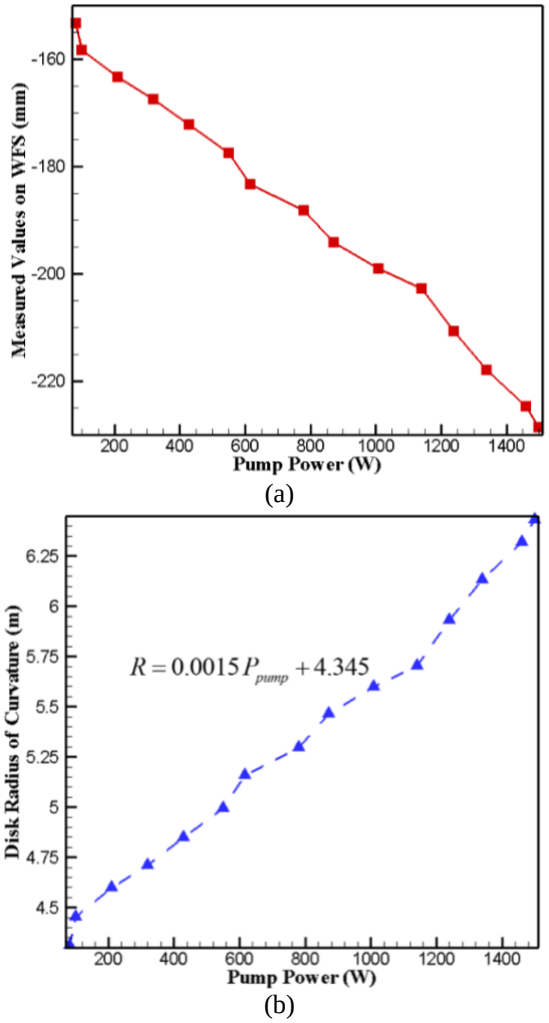

Fig. 3. The disk radius of curvature versus the pump power: (a) measured values on WFS and (b) disk radius of curvature.

Interpolating the measured values, the following relation between the disk's radius and pump power is achieved:

$$R = 0.0015\, P_{pump} + 4.345 \qquad (2)$$

where R is in meters and the P_{pump} is pump power in watts.

III. THE RESONATOR DESIGN

The laser oscillation occurs between two HR (high reflection) mirrors in cavity-dumped resonators. Between them, an electro-optical modulator (EOM) and a TFP are utilized to modulate the output mirror reflectivity so that the TFP acts as the output coupler. The fundamentals of utilizing a TFP as a reflectivity controllable mirror is illustrated in Fig. 4.

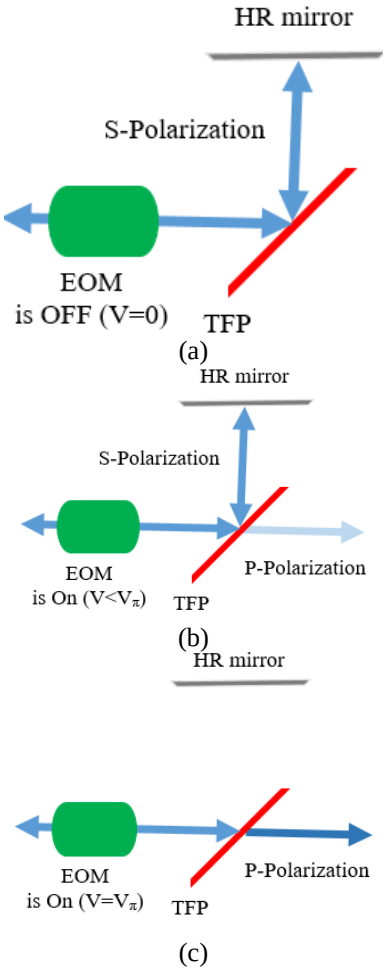

Fig. 4. A TFP with an EOM acting as a controllable reflectivity mirror. (a) The applied EOM voltage driver is off, (b) the applied voltage is less than V_π, and (c) V_π is applied to the EOM.

As shown in Fig. 4(a), when the EOM driver is off, s-polarization oscillates in the resonator while p-polarization is decayed. After enough time, the EOM acts, and the circulating beam polarization rotates, so some of the resonator internal power is extracted by the TFP.

Transmission and reflection of TFP depend on polarization, which inside the resonator is controlled by EOM voltage. As shown in Fig. 4(b), if the applied voltage to the EOM is less than the half-wave voltage V_π then the TFP acts as a partial reflection mirror. When the driving voltage is equal to V_π, the EOM and the TFP acts as a high transmission mirror, and all of the circulating power is extracted from the resonator. This method is well described in different laser textbooks [15].

The General configuration of a cavity-dumping resonator is illustrated in Fig. 5. The combination of a TFP and EOM acts as the laser output coupler mirror. A quarter-wave plate helps the system operate on the EOM at a lower operational voltage.

In terms of resonator design, this resonator configuration is a folded resonator used in cavity-dumping and many second harmonic generation setups and mode-locked lasers. Because of the oblique folding angle in the resonator, astigmatism in resonator characteristics should be considered in the resonator design. Astigmatic beams may have different transverse mode sizes in two orthogonal directions, reducing the mode overlap between the laser mode and pump area and leading reduction in the optical efficiency.

In the design procedure of the resonator, considering the variation of the disk's radius with the pump power, we treated the disk as a variable thermal lens inside the resonator.

Practical considerations for the defined industrial laser system were regarded in the resonator design. The most important is the overlap between the pumped region and the resonator modes. The laser transverse mode size should equal the pump spot diameter (7 mm) during all pumping powers, because, otherwise, the efficiency of the laser drops dramatically. Also, it may lead to a severe increase in the temperature of the un-depleted region of the pumped area damaging the disk.

According to the final aim of this work, the M^2 factor of the designed laser must be better than 24 such that the output beam could be coupled into a fiber with a diameter of 200 µm to be practical in industrial systems [4, 22]. The laser beam quality should remain almost constant during the pumping and does not change with variations of the disk's radius of curvature.

We always kept our eyes on the stability characteristics of the resonators, such that our resonators remained far enough from the stability boundaries. This point is very critical considering the mechanical stability of the

resonator. The $g_1 \times g_2$ stability coefficients of the resonator were restricted to intervals of 0.35 and 0.65. Finally, the transverse mode size within the resonator should match the entrance aperture of the electro-optic modulator by about 9 mm.

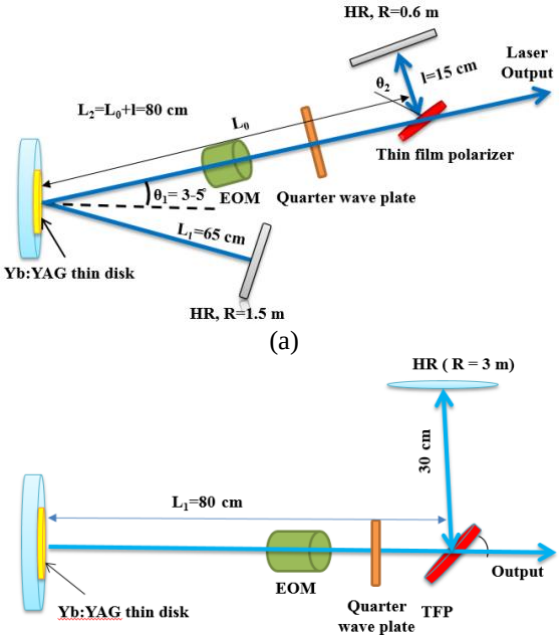

Fig. 5. Cavity-dumping resonators: (a) V-shaped and (b) L-shaped

To design and analysis of the resonator, we have used the LASCAD simulation software to model our resonators. With the mentioned constraints, we investigated the L- and V-shaped cavity-dumped resonators and optimized the cavity parameters in terms of beam quality and stable performance. Arrangements of L- and V-shaped cavities are shown in Fig. 5. Using LASCAD, the general properties of the resonator, such as mode sizes and stability criteria, can be extracted directly from the software. LASCAD uses a Gaussian mode algorithm to compute the mode structure in the laser cavity using complex ABCD matrices. The thermally loaded gain medium's temperature distribution, deformation, and stress are computed using Finite Element Analysis (FEA). For cases where wave optics effects are essential, the FEA results can alternatively be used as input for a physical optics code.

In the simulations, Yb: YAG medium's optical and mechanical properties are utilized [18]. We have approximated the pump profile distribution on the disk surface, with super-Gaussian distribution defined as

$$I(r) = I_0 \exp\left[-2\left(r/\omega\right)^{SG}\right] \tag{3}$$

with ω represents laser beam width and SG=10.

The Gaussian ABCD matrix gives the transverse eigenmodes of the resonator. The transverse mode structure represents sets of orthogonal eigenfunctions with different eigenvalues, so each mode oscillates independently. In this approach, the $M^2_{x,y}$, beam quality factor in x or y direction, is calculated by

$$M^{2}_{x,y} = \sum_{i=1}^{n}\left(2p_{x,y}+1\right)c_i \tag{4}$$

in which $p_{x,y}$ is the order of the i-th transverse mode in x or y-direction, and c_i is the relative contributions of the individual modes to the total power output, and n is the total number of modes [23].

Also, this approach uses the multimode rate equation to calculate the laser output power. In other words, the rate equations were solved independently for every transverse mode, the laser output power for i-th transverse mode is calculated separately, and the total average power of the laser is the sum of the power in all modes.

So, two coupled differential equations for $S_i(t)$, the photon numbers in the i-th transverse mode in the resonator, and $N(t)$, the laser upper-state population density, solved [23]:

$$\frac{\partial S_i(t)}{\partial t} = \frac{c\sigma}{n}\int_{\Omega} N S_i s_i dV - \frac{S_i}{\tau_c}, \tag{5}$$

$$\frac{\partial N(t)}{\partial t} = -\frac{c\sigma}{n} N S_c s_c - \frac{N}{\tau_f} + R_p \frac{N_{tot} - N}{N_{tot}} \qquad (6)$$

where n is the refractive index of the active medium, c is vacuum speed of light, R_p is the pump rate, σ is effective cross section of stimulated emission, τ_c is life time of laser photons in the cavity, τ_f is spontaneous fluorescence life time of upper laser level, N_{tot} is total active ion density. In this way the power output delivered by the individual transverse modes is [23]:

$$P_i = h\nu_l S_i(t) \frac{-Ln(R_{OC})}{t_{rtrip}} \left[1 - 0.5 Ln(R_{OC})\right] \qquad (7)$$

where R_{oc} is the reflectivity of the output mirror. The total output power is sum of output powers of all transverse modes.

Also, the temperature distribution in the active medium is calculated by solving the conduction equation in the active medium [24]

$$-\nabla.(\kappa(T)\nabla T) = Q(x, y, z) \qquad (8)$$

In this equation κ(T) is the thermal conductivity of Yb:YAG, and $Q(x, y, z)$ is the heat generation density in the active medium and is a portion of absorbed pump power. This equation is solved by FEM (finite elements method). More details on the boundary condition in the simulations were discussed in the LASCAD supporting documents [23, 24].

IV. Analysis and Discussion

According to the considerations for the resonator stated in the previous section, the optimal values of the resonator parameters should be determined.

The plot of the stability criterion $g_1 \times g_2$ for the L-shape and V-shape resonators over different resonator arm lengths is provided in Fig. 6. This figure made choosing the desired resonator very straightforward. The stability criterion $g_1 \times g_2$ of the resonator should be between 0 and 1 for stable resonators, with g_i parameter of mirrors defined as $g_i = 1 - L/R_i$. As its value approaches the borders of the stable regions, that resonator becomes more sensitive to misalignments of the optical elements. Evidently, the designed cavities have their stability criterion in the interval of 0.4 to 0.65, and thus suffer from minor misalignment sensitivity. Specifications of the selected resonators are shown in Fig. 5.

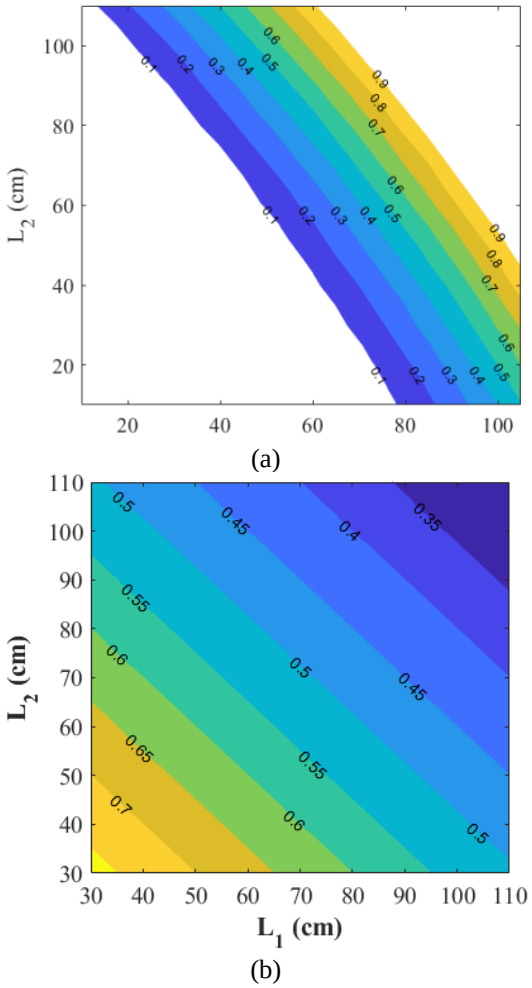

(a)

(b)

Fig. 6. Stability parameters of the dumped cavities scanned over different arm lengths for (a) V-shaped and (b) L-shaped resonators.

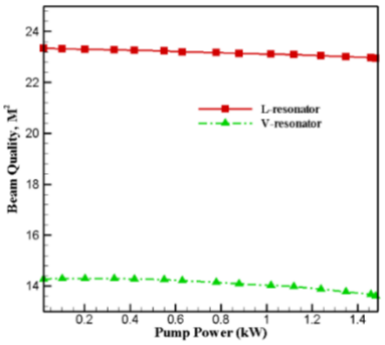

Fig. 7. Beam quality of the designed resonators versus pumping power.

The beam quality of the designed resonators concerning the pumping power is shown in Fig. 7. It is evident that the designed resonators have acceptable performance in terms of beam quality.

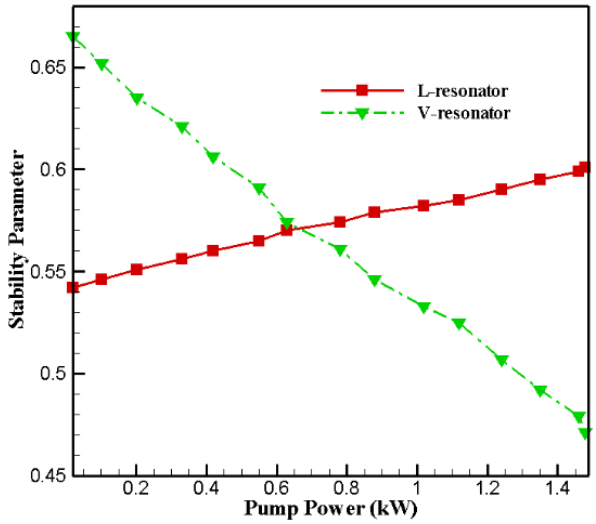

Fig. 8. Stability parameter of the designed resonators versus pumping power.

Another great point about the designed resonators is that the variations of beam quality during the pumping powers are negligible, which could also be considered a beneficial characteristic of the designed resonators. Figure 8 shows the stability parameter of the designed resonators as a function of the pumping power. As shown in Fig. 8, the resonator stability criterion remains in the previously considered interval of 0.35 and 0.65 in all pumping powers.

In Fig. 9 the V-shaped resonator's dependency on the laser beam's incident angle to the disk (Θ_1 in Fig. 5.) is shown. As shown in Fig. 9, changing this angle to 10 degrees does not significantly affect the mode properties, resonator stability, and laser beam astigmatism. The incidence angle of 3.5 degrees has been chosen based on the mechanical considerations in the mirrors' mounting.

The TEM_{00} mode size of the scanned resonators is shown in Fig. 10. To single-mode performance, the fundamental mode spot size must be slightly smaller than the pump spot so that higher-order modes cannot propagate within the resonator.

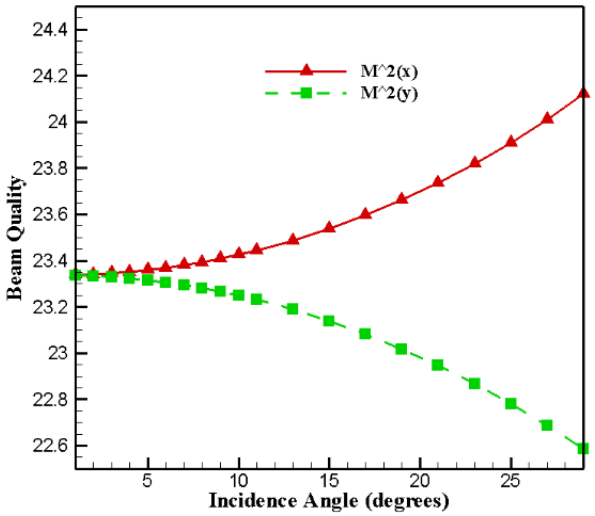

(a)

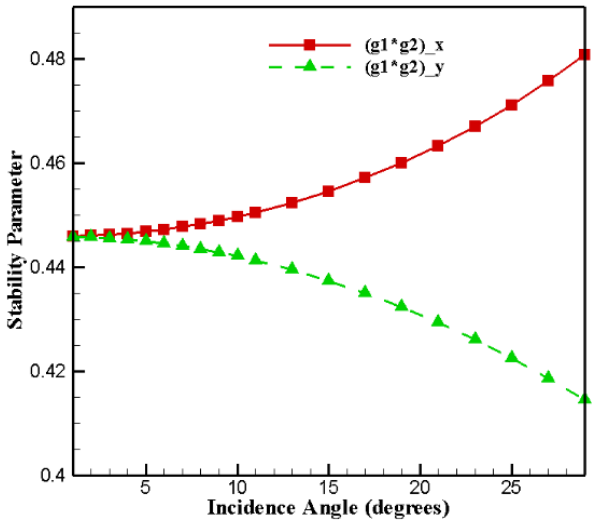

(b)

Fig. 9. The angle dependency of beam quality (a) and resonator stability (b) in V-shaped dumped cavity.

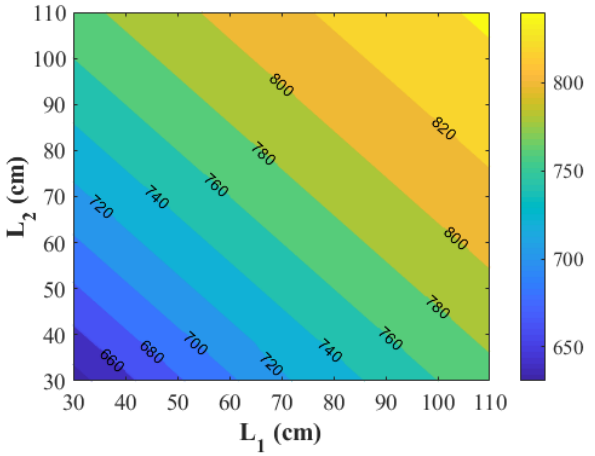

Fig. 10. TEM_{00} mode spot sizes (in μm) of the dumped cavities for L-shaped resonator.

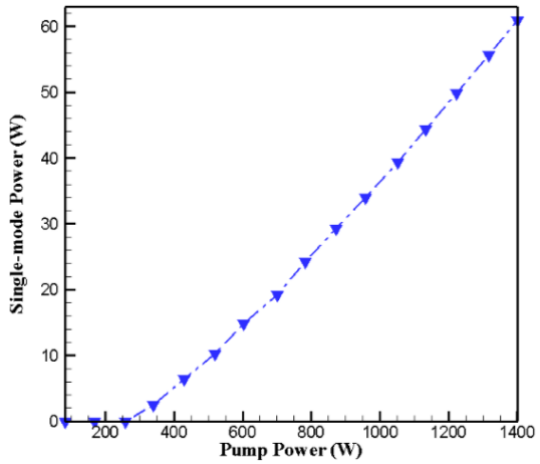

(a)

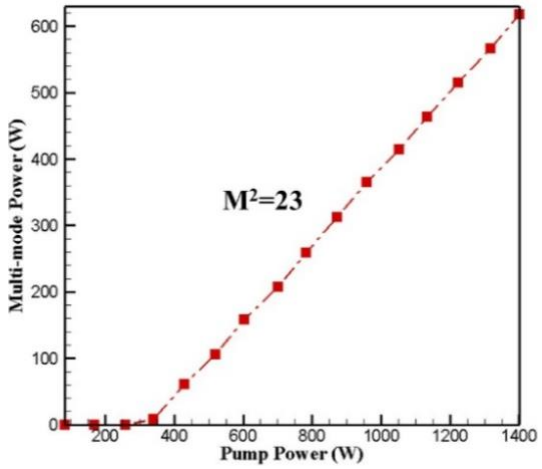

(b)

Fig. 11. The laser output power of dumped cavities for (a) single-mode and (b) multimode operation.

Figure 11 illustrates the output power of the L-shaped resonator for multimode (M^2=23) and single-mode operations. These data show good agreement with experimental values; in the lab, we have extracted about 0.58 kW output power from 1.4 kW of diode pump, which proves the validity of our simulation results.

In Fig. 12, the temperature distribution of the disk surface in the maximum pump power can be seen. It clearly shows the temperature profile of the disk surface in the pumped region and indicates the heating of the gain medium. This figure is in very good conformity with our experimental measurements.

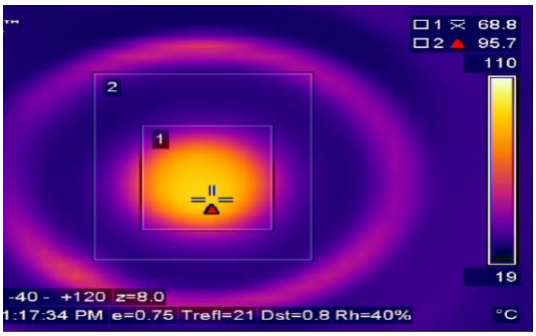

(a)

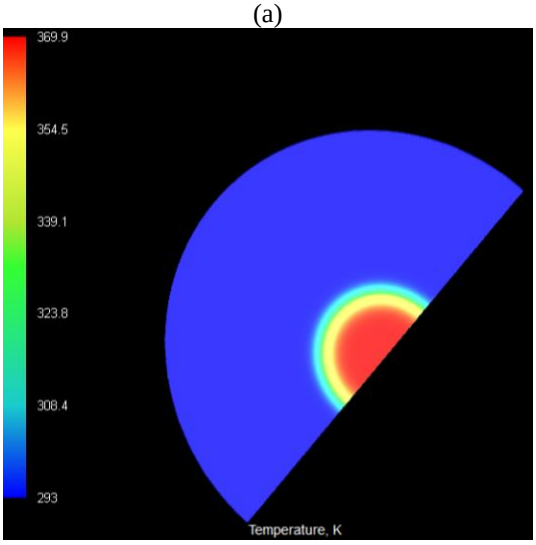

(b)

Fig. 12. (a) thermography of disk surface in maximum pump power and (b) simulation of temperature distribution of the disk surface.

V. CONCLUSION

Based on the measured values for the variations of the radius of curvature of the thin-disk active medium during the diode pumping, two kinds of cavity-dumped resonators were designed and investigated. Considering the potential industrial applications of this laser, the design procedure of those cavities was done with some constraints imposed on the transverse mode sizes, beam quality, and resonator stability. The findings of our simulation prove that the L-shape resonator has better performance in terms of misalignment sensitivity, whereas the V-shaped resonator has better beam quality. Our results prove that both kinds of resonators could be used to achieve high-power nanosecond pulses.

Additionally, astigmatism, due to the oblique angle of incidence in the resonance path, has

been considered and compensated without the need to use a mode-limiting aperture.

ACKNOWLEDGMENT

The authors would appreciate Mr. Mahdi Bakhtiary with INLC, for contributing to the experiments.

REFERENCES

[1] A. Sennaroglu, *Solid-state lasers and applications*, Rochester, N.Y: CRC Press, Ch. 1, 2017.

[2] W.M. Steen and J. Mazumder, *Laser material processing*, Springer Science and Business Media, 2010.

[3] U. Brauch, C. Röcker, T. Graf, and M. Abdou Ahmed, "High-power, high-brightness solid-state laser architectures and their characteristics," Appl. Phys. B, Vol. 128, pp. 58 (1-32), 2022.

[4] B. Schmidt and M. Schaefer, "Advanced industrial laser systems and applications," Proc. of SPIE, Vol. 10525, High-Power Laser Materials Processing: Applications, Diagnostics, and Systems VII, 1052502 (1-13), 2018.

[5] R. Paschotta, "Q-switching," rp-photonics.com/q_switching.html., 2011.

[6] R. Paschotta, "Field guide to laser pulse generation," Ed: SPIE press Bellingham, 2008.

[7] C. Stolzenburg, A. Voss, T. Grafa, M. Larionovb, and A. Giesenc, "Advanced pulsed thin disk laser sources," SPIE, Vol. 6871 68710H-1, 2008.

[8] L. Tarra, A. Olek, V. Stummer, T. Flöry, A. Baltuska, and A. Kugi, "A stochastic nonlinear model of the dynamics of actively Q-switched lasers," ArXiv preprint arXiv:2205.08460, 2022.

[9] J. Brooks, G. Bonner, A. Kemp, and D. Stothard, "Stability of Q-switched 2 μm lasers," OSA Continuum, Vol. 3, pp. 568-579, 2020.

[10] S. Radmard, A. Moshaii, and K. Pasandideh, "400 W average power Q-switched Yb:YAG thin-disk-laser," Scientific Reports, Vol. 12, pp. 16918 (1-10), 2022.

[11] S. Schad, T. Gottwald, V. Kuhn, M. Ackermann, D. Bauer, M. Scharun, M. Scharun, and A. Killi, "Recent development of disk lasers at TRUMPF," Solid State Lasers XXV: Technology and Devices, p. 972615, 2016.

[12] L. Dai, R. Liu, X. Li, F. Gong, X. Lei, H. Li, S. Deng, Q. Lv, T. Sun, F. Teng, G. Li, and Y. Jin, "High-efficiency, high-repetition-rate cavity-dumped Q-switched Yb: YAG thin-disk laser based on a 72-pass pump module," Opt. Express, Vol. 30, pp. 19629-19638, 2022.

[13] C. Fries, M. Weitz, C. Theobald, J. Bartschke, and J.A. L'huillier, "Cavity-dumped Yb: YAG ceramic in the 20 W, 12 mJ range at 6.7 ns operating from 20 Hz to 5 kHz with fluorescence feedback control," Appl. Opt., Vol. 55, pp. 6538-6546, 2016.

[14] L. Dai, R. Liu, F. Gong, X. Li, S. Deng, Y. Jia, Y. Jin, and G. Li, "Cavity-Dumped Nanosecond Thin-Disk Laser with High Average Power," Chin. J. Lasers, Vol. 48, p. 1301002, 2021.

[15] W. Koechner, *Solid-state laser engineering*, Round Hill, VA: Springer, Ch. 10, 2013.

[16] S. Arabgari, M. Aghaie, S. Radmard, and S.H. Nabavi, "Thin-disk laser resonator design: The dioptric power variation of thin-disk and the beam quality factor," Optik, Vol. 185, pp. 868-874, 2019.

[17] M. Shayganmanesh, M. Daemi, Z. Osgoui, S. Radmard, and S.S. Kazemi, "Measurement of thermal lensing effects in high power thin disk laser," Opt. Laser Technol., Vol. 44, pp. 2292-2296, 2012.

[18] H. Injeyan, and G. Goodno, *High Power Laser Handbook*, New York: McGraw-Hill, 2011.

[19] M. Moslehian, S. Arabgari, E. Nahvifard, and S. Radmard, "Measurement of gain coefficient and resonator internal loss in Yb: YAG thin-disk-laser," Opt. Laser Technol., Vol. 118, pp. 151-158, 2019.

[20] S. Radmard, S. Arabgari, and M. Shayganmanesh, "Optimization of Yb: YAG thin-disk-laser design parameters considering the pumping-light back-reflection," Opt. Laser Technol., Vol. 63, pp. 148-153, 2014.

[21] S. Radmard, S. Arabgari, M. Shayganmanesh, and S. Kazemi, "Investigation on back-reflected pumping light in high-power quasi-end-pumped Yb: YAG thin-disk lasers," IEEE

J Quantum Electron, Vol. 48, pp. 1137-1143, 2012.

[22] TruMatic 7000| TRUMPF. Available: https://www.trumpf.com/en-CN/products/lases/short-and-ultrashort-pulse-laser/trumicro-series-7000.

[23] A. Konrad. (2020). Dynamic Analysis of Multimode and Q-Switch Operation (DMA). Available:lascad.com/lascad_documentation.php.

[24] A. Konrad. (2020). The FEA Code of LASCAD. Available: las-cad.com/lascad_documentation.php.

Saeid Radmard received his M.Sc. degree in laser physics in 2005. The topic of his MSc thesis was thermal lensing effects in fiber-coupled end-pumped lasers. Since then, he had been a member of solid-state laser department of Iranian National Laser Center (INLC). He is currently a PhD candidate in atomic and molecular physics in Tarbiat Modares University, Tehran, Iran, and works on pulsed thin-disk lasers design and fabrication.

His current research interests include theoretical and experimental studies on solid-state lasers, laser applications, and computational physics.

Dr. Ahmad Moshaii received his PhD degree from Physics Department of Sharif University of Technology, Tehran, Iran, in 2004 in the field of sonoluminescence. Then he worked at Institute for Studies in Theoretical Physics and Mathematics (IPM) as a Postdoc researcher with concentration on Resistive Plate Chamber detectors. He then joined Tarbiat Modares University as an associate professor in 2008 and established the Nano Optics Lab. in Physics Department of Faculty of Basic Sciences. Currently, his research interest concentrates on plasmonic materials for solar harvesting systems including solar cells and photoelectrochemical water splitting cells, and biosensors.

Mohammad Abazari was born in 1984 in Khoy city, Iran. He continued his study in Physics and completed his MSc thesis on the interaction of laser with human fat tissue and graduated in M.Sc. in molecular physics from Amir Kabir University of Technology in 2014.

He then continued to collaborate as a researcher in some highly prestigious research centers in the country. He now does his research career in Iranian National Center for Laser Sciences and Technologies, Tehran, Iran.